Evolution of the alpine Critical Zone since the Last Glacial Period using Li isotopes from lake sediments

Xu (Yvon) Zhang [a,d,f,*], Manon Bajard [b,e], Julien Bouchez [a], Pierre Sabatier [b], Jérôme Poulenard [b], Fabien Arnaud [b], Christian Crouzet [c], Marie Kuessner [a], Mathieu Dellinger [b], Jérôme Gaillardet [a]

[a] Université Paris-Cité, Institut de physique du globe de Paris, CNRS, F-75005 Paris, France
[b] EDYTEM, Université Savoie Mont-Blanc, CNRS, 72376 Le Bourget du Lac, France
[c] Université Savoie Mont Blanc, Université Grenoble Alpes, CNRS, IRD, Université Gustave Eiffel, ISTerre, Le Bourget du lac, France
[d] Université de Strasbourg, CNRS, 1 rue Blessig, 67084, Strasbourg, France
[e] Department of Geosciences, University of Oslo, Oslo, Norway
[f] Department of Geosciences, Utrecht University, 3584 CB Utrecht, the Netherlands

ARTICLE INFO

ABSTRACT

Comprehending and predicting the way humans affect the Earth's Critical Zone remains a challenge. An understanding of the past changes resulting from human and non-human influences in the dynamics of the Critical Zone is crucial. Here, we use a retrospective approach to address this question based on a new lithium (Li) isotope record from the Late Glacial Period to the present from a pre-Alpine lake sediment sequence (Lake La Thuile, France). Coupled with the lake sediment archive, the investigation of present-day soils in the lake catchment suggests that lake sediments are not necessarily recording the erosin of topsoil in the catchment. Our findings indicate that soil particles can be sorted during transportation to the lake, with finer particles being preferentially mobilized, highlighting the influence of fine particle transport on the Li isotope signature of soils and lake sediments. Characterized by low Li isotope signatures, changes in weathering signatures in lake sediments can be amplified by the combined effect of soil development and selective transport. In the La Thuile catchment, soil development was limited during the Late Glacial Period, whereas it became a dominant process during the Holocene climatic optimum together with enhanced selective transport of fine particles. Human activities since 3,000–4,000 yr cal BP induced a strong perturbation hindering both soil formation and selective transport by reinforcing erosion rates. After a period of topsoil destruction caused by intense deforestation and agriculture, lake Li isotopes record the evolution of soil profiles associated with changes in agricultural practices.

1. Introduction

The spread of agriculture over the Holocene has resulted in deforestation, shifts in vegetation types, and enhanced physical erosion (Ruddiman, 2013; Stephens et al., 2019). These factors threaten the sustainability of Earth's Critical Zone (CZ, the thin layer of the planet spanning from bedrock to land surface encompassing the hydrosphere and the biosphere), and hence of civilizations (*e.g.*, Gaillardet et al., 2018; Montgomery, 2007). The CZ evolution over time is influenced by various factors with human activities progressively becoming the most powerful one, which has led scientists to coin the term "Anthropocene" designating a new geological epoch characterized by the rise of human

activities as a global factor of the Earth's surface evolution (Gibbard et al., 2022; Steffen et al., 2018). To comprehend and forecast the response of the CZ to the pressures of climate change and escalating human impacts, it is crucial to gain insight into these aspects and to understand how each of these influencing factors affects the CZ. Unravelling these aspects and their impacts on the CZ, and thus the sustainability of human societies in the recent past of the Earth, is a scientific challenge of paramount importance.

Lake sediments are watershed-integrated archives of environmental conditions and provide unique insight into past changes in soil dynamics (Bajard et al., 2017b; Jenny et al., 2019). Lake sediment geochemical records are valuable tools for reconstructing CZ evolution and for

exploring the complex interplays between human activities, geo-dynamics, and climate over centennial to millennial timescales (Arnaud and Sabatier, 2022; Nantke et al., 2021; Rapuc et al., 2022). Lithium (Li) isotope composition is an innovative tracer for reconstructing past weathering processes. Li is a trace element primarily carried by silicate minerals (*e.g.*, Pogge von Strandmann et al., 2020; Rudnick et al., 2004; Song et al., 2021). During silicate weathering, the lighter Li isotope (^{6}Li) is preferentially incorporated into soil-forming phases such as clays, leaving soil- and river- solutions enriched in the heavier Li isotope (^{7}Li) (Huh et al., 1998). The Li isotope composition (δ^7Li) of terrigenous sediments therefore reflects the extent of secondary mineral formation and thus pedogenetic processes (Dellinger et al., 2017; Dosseto et al., 2015). Furthermore, past local variations in soil formation rates and weathering processes can be recorded in the δ^7Li of the detrital material accumulated in lakes (Rothacker et al., 2018).

Here we study pre-Alpine soils and associated lake sediments that have been previously well characterized for several Holocene paleo-environmental proxies including pollen records, mineral and organic geochemistry, and sedimentary DNA (Bajard et al., 2017a, 2016; Giguet-Covex et al., 2019). Previous studies suggest that the rates of soil processes were disrupted by the settlement of humans in the catchment. Here we attempt to extract new information from the soil and sediment Li isotope data, focusing on historical variations in soil development and soil erosion.

Properly interpreting detrital archives of soil processes relies on understanding the soil material contributing to the sediment and its transport mechanisms. Recent studies have highlighted variations in sediment geochemistry under different hydrological conditions, favouring the transportation of finer particles with geochemical char-acteristics similar to clay minerals (*e.g.,* Kim et al., 2018), leading to their accumulation in sediment deposits (Ma et al., 2015). While past changes in soil formation can impact the sediment record (Rothacker et al., 2018), it remains uncertain whether variations in sediment transport and associated transformations would play a significant role in setting the composition of detrital sediments.

The preferential mobilization of fine particles during soil erosion is well-documented (Morgan, 2009 and references therein). Lessivage, the downward migration of particles in soil profiles involves the loss of fine particles (eluviation) from the upper soil horizons and their accumula-tion in deeper soil horizons (illuviation) (Quénard et al., 2011). Such translocation of fine particles is part of soil formation processes, particularly in humid climates (Buol et al., 2011). Nevertheless, the potential impact of this transport on the geochemical signatures in lake sediments, remains a knowledge gap.

Recent studies have extensively examined the selective transport of fine particles within and from soils (Bern et al., 2011; Jin et al., 2010; Noireaux et al., 2021; Steinhoefel et al., 2021), emphasising the importance of the preferential export of fine particles (<1 μm), which have distinct compositions compared to bulk soil. This selective export results in the loss of elements typically considered immobile during weathering (*e.g.*, Al, Ti, Zr; Jin et al., 2010; Kim et al., 2018). Regarding Li isotopes, the fine particle fraction, characterized by low δ^7Li values, is preferentially exported from soil profiles (Steinhoefel et al., 2021). Consequently, detrital sediments in lakes may reflect at least in part selective transport, with finer particles being preferentially mobilised and enriched in the lake deposit (Dietze et al., 2014; McLaren and Bowles, 1985). This suggests that variations in lake sediment geochemistry are not solely influenced by temporal changes in the composition of the bulk (or surface) soils, but also by how selective export and sedimentation of grain size fractions varies as a function of climate and human forcing. If selective transport were significant, any increase in its magnitude within a catchment could result in (1) an elevated δ^7Li signature in the remaining soil material (Steinhoefel et al., 2021) and (2) a depleted δ^7Li signature in the lake deposit, possibly biasing the interpretation of the sedimentary record.

This potential complexity calls for new studies aiming at

understanding how the evolution of soil erosion and weathering pro-cesses are recorded in detrital sediments by integrating lake δ^7Li records and examining soils within the corresponding drainage basin. This study presents δ^7Li values and elemental geochemical data from pre-Alpine soils and associated lake archives. The δ^7Li signature in detrital sedi-ments is influenced by both grain size sorting and chemical weathering reactions (Dellinger et al., 2014; Zhang et al., 2022). Consequently, it can serve as a tool to examine the impact of either selective transport or changes in soil development, providing that the other effect is accounted for. We first validate the use of Li isotopes in sediments for tracking past changes and then examine the CZ evolution of the lake La Thuile watershed since the Last Glacial Period. To support our interpretations, we employ additional geochemical tools such as element ratios and microscopic imaging to disentangle the impacts of selective transport and weathering on the geochemical signatures in soils and sediments. Ultimately, we establish that variation in δ^7Li within the lake sediment record is a powerful proxy to investigate the evolution of the CZ at the catchment scale.

2. Study site and sample material

Lake La Thuile is a small (0.06 km^2) glacial lake in the Northern French Alps (Fig. 1A). The catchment is primarily underlain by calcar-eous formations associated with Cretaceous marls, shales, and lime-stones, with sparse Quaternary glacial deposits in the northwest (Fig. 1B). This lake has a maximum depth of 8 m with an intermittent narrow outflux in the north and is fed by two ephemeral streams during snowmelts and long rainfall episodes. The present catchment is domi-nated by forests, except for lakeside grasslands (Fig. 1C). In April 2010, an 18-metre-long sediment sequence was collected from the deepest part (8 m) of the lake (45°31′48.8″ N, 6°03′23.6″ E) using a Uwitec platform and coring devices. The details of sampling and the analyses for geochemistry, chronology, and palynology were previously reported for the upper 6 m corresponding to the Holocene by Bajard et al. (2016) and 12 m for the Late Glacial Period by Banjan et al. (2023). The sediment sequence (THU10, IGSN:IEFRA00BB, www.geosamples.org) consists of two overlapping cores (THU 10–1 and THU 10–2), with a chronology established through nineteen ^{14}C AMS measurements of terrestrial macroremains, paleomagnetic data, and short-lived radionuclides (Fig. S1). Notably, no plant macroremains were collected between 11.62 m and the bottom of the sequence *ca.* 18 m. The deepest radio-carbon date ranges between 16,160 and 16,600 yr cal BP. The base of the sedimentary sequence, located 650 cm below this level, contains crystalline material of glacial origin. The earliest laminated lacustrine sediments were deposited immediately after glacial retreat, according to cosmogenic dating (Roattino et al., 2022; Wirsig et al., 2016). While the ages of the deeper sediment core section obtained from extrapolation may appear too old compared to the age derived from cosmogenic dating, these samples are not discussed in detail in this article.

Two soil profiles (THU01 and THU02) were sampled in the northern part of the catchment under a spruce forest. THU01 (5 horizons, 45°31′55.290″N, 6° 4′1.464″E) was sampled down to 70 cm, and THU02 (4 horizons, 45°31′53.124″N, 6° 4′1.608″E) was sampled down to 80 cm (Figs. 1 and 2). Both profiles are cambisols and have been previously described by Bajard et al. (2017a). THU01 is a clay-loam soil with a blocky structure having an acidic pH ranging from 4.5 to 5.5. Charcoals are abundant between depths of 20 to 70 cm, and rust patterns are visible in the deepest horizons, with bedrock not reached at 70 cm depth. THU02 is developed on carbonate rocks, although its upper ho-rizons are carbonate-free. Its pH ranges from acidic to neutral, except in the C horizons where the matrix is carbonated. The structure is blocky, and the texture is silt loam. Both profiles are in close proximity and can be considered to have developed over the same parent material. A bedrock sample was collected from the outcrop underlying profile THU02, corresponding to a fine-grained carbonate formation associated with shale, assumed to be representative of the marine sedimentary
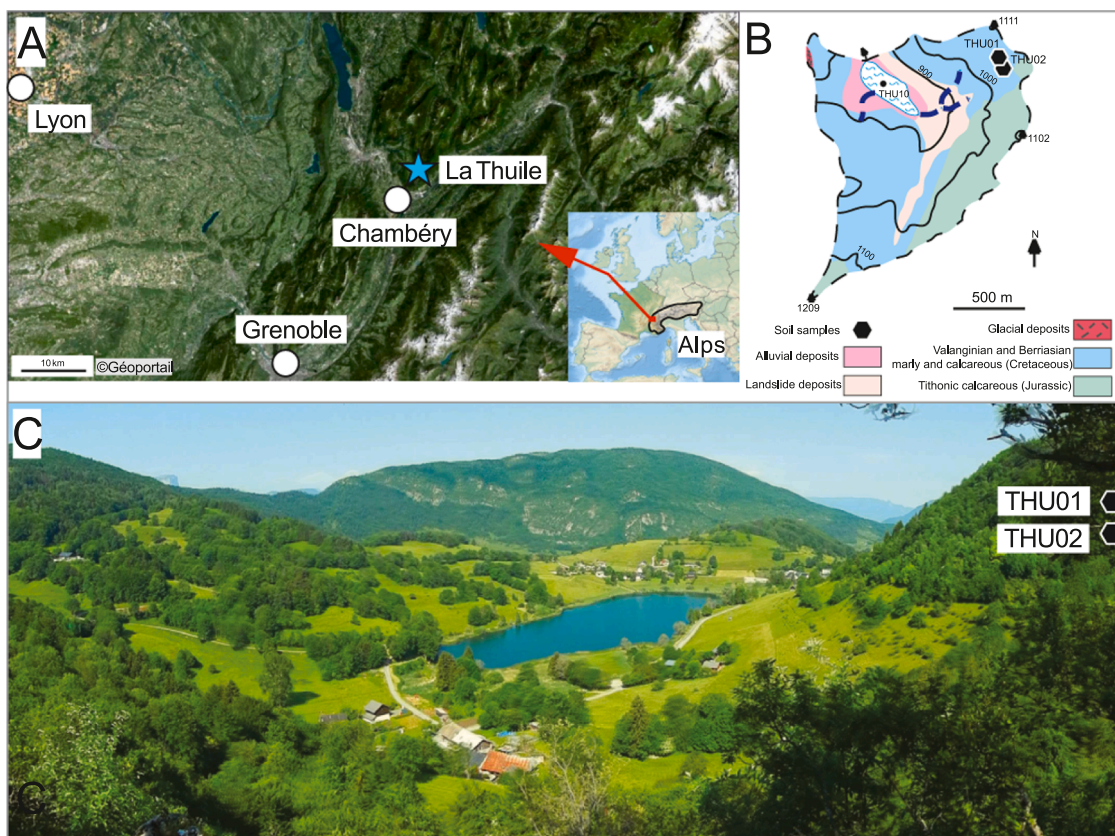
Fig 1. The La Thuile catchment: (A) map of the location of Lake La Thuile; (B) simplified geological map of the La Thuile catchment and the sample locations; and (C) a view of the lake from the south shore. Figure modified from Bajard et al. (2016, 2017b).

rocks making up the catchment bedrock.

3. Analytical methods

The grain size of Lake La Thuile detrital material during the Holocene period was previously reported by Bajard et al. (2016). In this study, additional grain size analyses on soil samples have been performed to complement the current lacustrine dataset. Fifty-milligram aliquots of soil samples were dispersed following ultrasonication in a sodium hexametaphosphate solution. The grain size distribution of the resulting suspension was then measured using a laser granulometer LS Coulter 320 at École Normale Supérieure (Paris, France). The grain size distributions of the two soil profiles are illustrated in Fig. S2.

Imaging analyses were performed for selected sediment and soil samples at the Electron Microscopy Centre at Utrecht University (Utrecht, Netherlands). Samples were attached to carbon stickers and coated with 5 nm platinum-palladium prior to analyses using a Zeiss Gemini 450 scanning electron microscope (SEM) equipped with an energy dispersive X-ray spectroscopy (EDX) for elemental analysis.

Lithium isotopic analyses were carried out at the PARI platform of the Institut de Physique du Globe de Paris. Soil and lake sediment samples were gently ground in an agate mortar and air dried at ~50 °C before being digested using a mixture of HF-HNO$_3$ (Kuessner et al., 2020) in Teflon beakers. The resulting solution was then repeatedly evaporated and redissolved in concentrated HCl and HNO$_3$ solutions until it was clear. Silicon content was measured using alkali fusion with NaOH (Georg et al., 2006). Major and trace elements were analysed using ICP-Q-MS, and the analytical uncertainties were controlled to be below 5% for major elements and 10% for trace elements by analysing certified reference materials (BHVO-2, JB-2, and Till-1), which were treated following the same digestion and analysing protocols. Procedure blanks yielded signals below the instrumental detection limits of

ICP-Q-MS.

A total of 17 sediment samples, ranging from a depth of 17.36 m to the modern sediment (0.4 m), were analysed for Li isotopes. A double-step separation protocol using a 1-ml column (BioRad, AG50W–X12, 200–400 mesh) was employed to separate Li from the sample matrix (Zhang et al., 2021). The purified samples were measured for Li isotopes using a Thermo Fisher Neptune Plus MC-ICP-MS. The pure Li standard solution IRMM-016 was routinely measured to monitor the instrumental stability. The signal of the procedural blank on the MC-ICP-MS was indistinguishable from blank solutions, registering no effect on Li isotope measurements. The Li isotopic composition (δ^7Li) is defined as the deviation of the ^{7}Li/^{6}Li ratio compared to a reference material NIST RM-8545, commonly referred to as L-SVEC:

$$\delta^7\text{Li} = \left[\frac{\left(^7\text{Li}/^6\text{Li} \right)_{\text{sample}}}{\left(^7\text{Li}/^6\text{Li} \right)_{\text{L–SVEC}}} - 1 \right] \times 1000 \qquad (1)$$

Several samples were duplicated for δ^7Li analyses yielding differences smaller than 0.2 ‰. Five reference materials were routinely processed together with samples to assess for the quality of the protocol. The measurement results NASS-6 (δ^7Li = 30.99 ± 0.47 ‰, 2 s.d., n = 4), BHVO-2 (δ^7Li = 4.55 ± 0.45 ‰, 2 s.d., n = 2), SRM-2709a (δ^7Li = −0.57 ± 0.56 ‰, 2 s.d., n = 2), TILL-1 (δ^7Li = 6.27 ± 0.25 ‰, 2 s.d., n = 2), and JB-2 (δ^7Li = 4.61 ± 0.75 ‰, 2 s.d., n = 2) align with previously reported values (Kuessner et al., 2020; Weynell et al., 2017). The highest standard deviation from the reference material measurement (0.75 ‰) is used as the repeatability of our Li isotope measurements.

4. Results

The geochemical results, lake chronology, and inferred lake
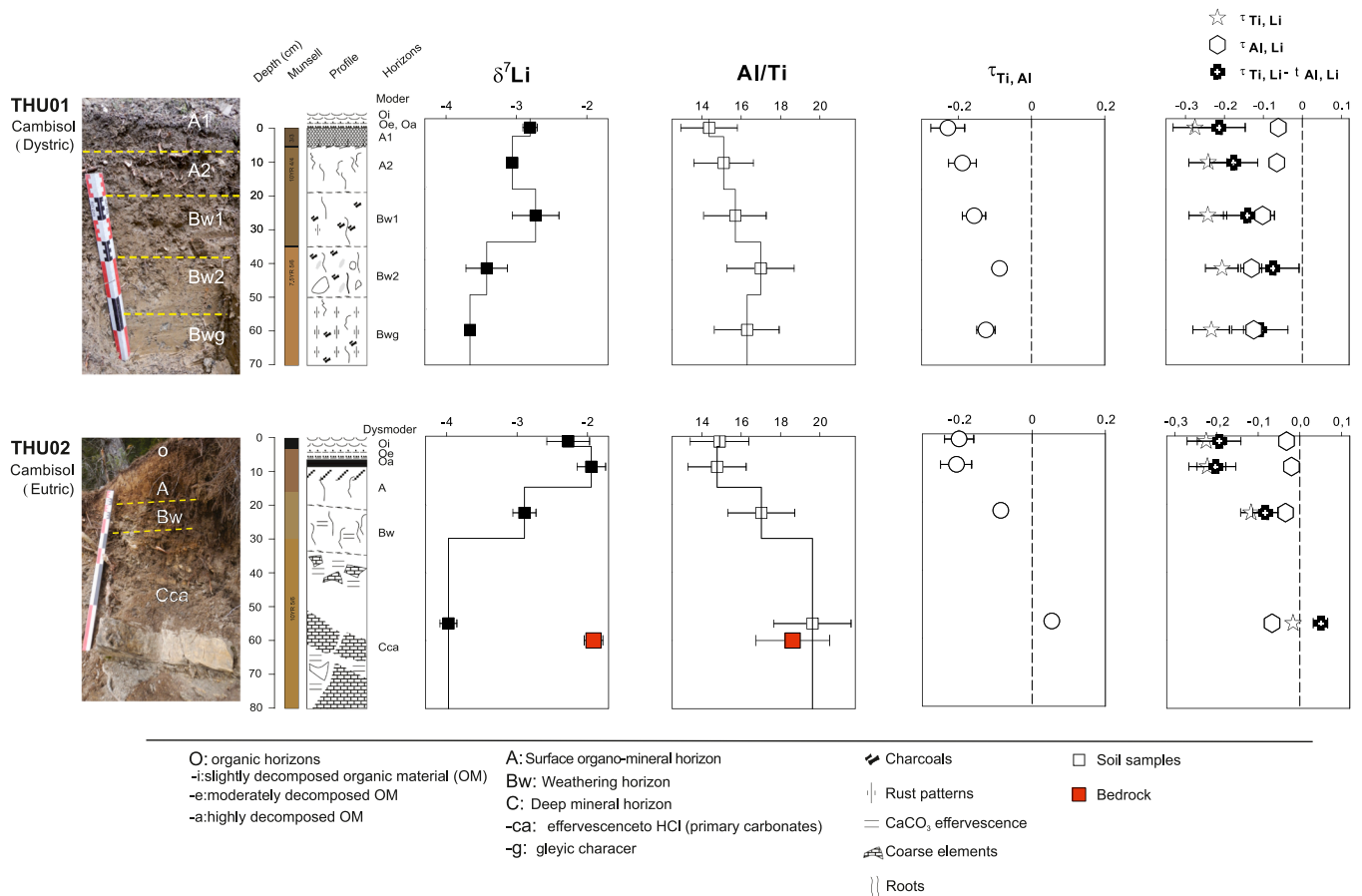
Fig 2. The two La Thuile soil profiles investigated in this study: pedogenic information (photo, colour, texture) and geochemical data, including δ^7Li, Al/Ti ratio, and mass transfer coefficients. Soil profiles are from Bajard et al. (2017b).

Table. 1

Major and trace element concentrations, δ^7Li values, and Al/Ti ratios of soil, bedrock, and lake sediment samples of the La Thuile catchment as well as ^{14}C ages and inferred sedimentation rate for lake sediments.

Sample name	Depth (m)	δ^7Li (‰)	2 s.d.	Li (ppm)	SiO$_2$ (%)	K$_2$O (%)	Al$_2$O$_3$ (%)	Ti$_2$O (%)	Zr (ppm)	Al/Ti (g/g)	Ages (cal BP)	Sed. Rate (mm/yr)
Lake sediments												
THU11-P2-a	0.40	−4.05	0.17	62	35.72	2.78	10.09	0.43	64	20.97	58	3.704
THU10–02-A1-a	1.60	−4.89	0.19	51	32.64	2.20	8.01	0.40	60	17.65	687	2.222
THU10–01-B1-a	2.96	−4.42	0.10	72	38.28	3.09	11.67	0.74	110	13.87	887	11.111
THU10–01-C1-b	4.33	−2.23	0.26	62	68.17	2.41	9.27	0.57	87	14.42	1309	1.351
THU10–02-B2-b	4.48	−2.84	0.31	35	44.17	1.19	4.89	0.33	60	13.23	1427	1.087
THU10–01C1a-129–130	4.69	−5.76	0.10	47	42.35	2.66	10.58	0.39	59	24.14	1697	0.581
THU10–02C1a-32–33	5.02	−6.64	0.09	44	31.90	2.59	10.35	0.34	54	26.75	2712	0.203
THU10–02-C1-a	5.10	−7.07	0.19	44	26.18	1.82	7.08	0.19	33	32.45	3202	0.161
THU10–02C1a-79–80	5.25	−5.82	0.22	22	30.15	1.50	5.41	0.21	31	22.46	4277	0.122
THU10–02C1a-110+111	5.41	−5.37	0.15	4	19.00	0.33	1.11	0.04	6	21.97	5643	0.106
THU10–02-C1-a	5.57	−6.18	0.21	7	10.72	0.42	1.44	0.07	10	19.30	7241	0.099
THU10–02C1a-169+170	5.70	−3.76	0.18	3	1.80	0.21	0.66	0.03	4	19.54	8587	0.101
THU10–02C1a-206–209	5.89	−4.49	0.20	19	12.42	1.39	4.24	0.20	25	18.57	10,278	0.130
THU10–02-D1-b	7.44	−3.68	0.05	37	29.25	2.39	7.38	0.35	54	18.55	12,930	0.330
THU10–02-E1-b	9.32	−4.03	0.29	43	28.91	2.21	6.92	0.33	53	18.57	14,640	1.408
THU10–01-G1	13.09	−3.61	0.28	53	33.14	3.27	9.63	0.44	70	19.14	17,492	1.316
THU10–02-I1-b	17.36	−3.74	0.23	35	27.70	2.24	6.30	0.35	50	15.86	20,746	1.316
Soils and bedrock												
TH01_1	0–5 cm	−2.81	0.10	61	67.39	2.41	10.55	0.65	99	14.37		
TH01_2	5–20 cm	−3.06	0.07	68	75.75	2.70	11.76	0.69	104	15.11		
TH01_3	20–30 cm	−2.73	0.33	71	77.63	2.68	12.89	0.73	110	15.70		
TH01_4	30–50 cm	−3.42	0.29	77	76.84	3.04	14.44	0.75	112	17.00		
TH01_5	50–80 cm	−3.66	0.04	75	77.22	3.06	14.01	0.76	120	16.30		
THU02_1	0–3 cm	−2.27	0.30	26	26.23	1.28	4.35	0.26	39	14.90		
THU02_2	3–15 cm	−1.95	0.20	54	66.70	2.29	9.03	0.54	90	14.78		
THU02_3	15–30 cm	−2.90	0.16	60	64.09	2.32	10.17	0.53	96	17.02		
THU02_4	30–40 cm	−3.97	0.12	55	52.18	2.53	9.51	0.43	72	19.62		
THU02_R	Bedrock	−1.91	0.13	38	52.21	1.83	6.24	0.30	52	18.62		

sedimentation rates are summarized in Tables 1 and S1. The two soil profiles display noteworthy δ^7Li variations ranging from −3.97 to −1.95 ‰ with similar trends of higher δ^7Li values toward the soil surface (Fig. 2). Conversely, the Al/Ti ratio (g/g) exhibits an opposing pattern,

increasing with depth in both soil profiles. Compared to deep soil material, the bedrock sample collected at THU02 has a lower Al/Ti (within the margin of error) and an elevated δ^7Li (Fig. 2).

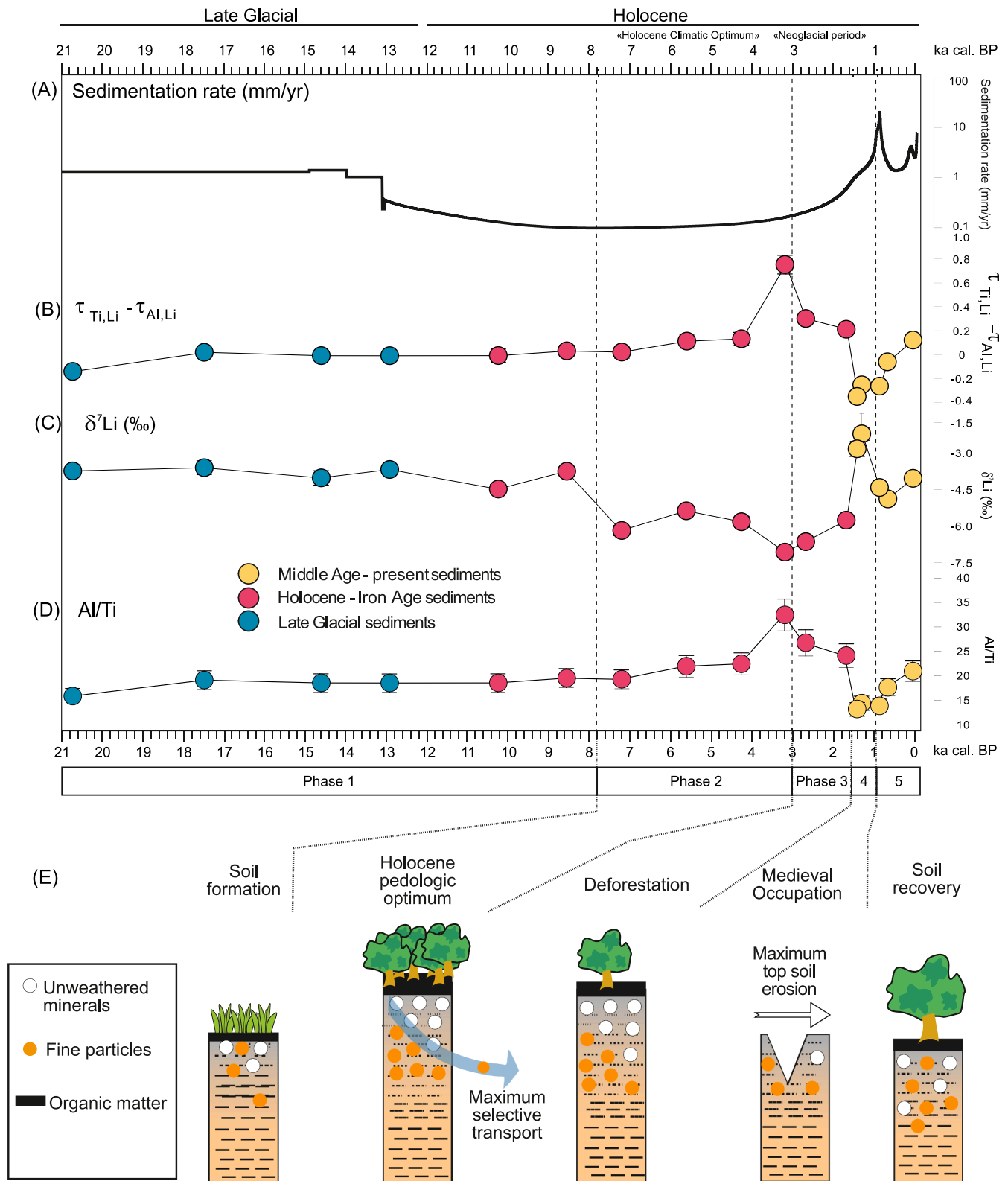Lake sedimentation rates varied from moderate (~1 mm/yr) during

Fig 3. Temporal variations in sedimentation rates (A), selective transport of fine particles indexed by $\tau_{Ti,Li}$-$\tau_{Al,Li}$ (B), sediment δ^7Li (C), and Al/Ti (D) in Lake La Thuile since the Late Glacial Period; (E) Sketch representing the history of soil development in the La Thuile catchment over the Late Glacial and Holocene periods. Fig. 3E modified from Bajard et al. (2017b) and Arnaud and Sabatier (2022).

the Late Glacial Period to low values (~0.1 mm/yr) in the Holocene (Fig. 3A). An abrupt increase in sedimentation rates (~11 mm/yr) occurred around the Middle Age (~1000 yr cal BP), followed by a period of reduced albeit still high rates (~3 mm/yr) in recent history. The corresponding δ^7Li varies accordingly (Fig. 3C), *i.e.*, remained stable from the Late Glacial Period to the Early Holocene at ~−4 ‰ and gradually decreased to reach its minimum value over the record (δ^7Li = −7.1 ‰) at ~3200 yr cal BP. Afterward, a slow increase was observed followed by a more significant rise in δ^7Li at approximately 1300 yr cal BP up to −2.2 ‰, a value close to the modern surface soil horizon (Fig. 2). Later, the δ^7Li in lake sediments gradually decreased until it

reached the value of recently deposited sediments (−4.0 ‰). The Al/Ti ratios in the lake sediments display a temporal variation opposite to that of δ^7Li (Fig. 3D). The concentration ratios between individual REEs and Ti are similar between the soil profiles and lake sediments (Fig. S3).

5. Discussion

5.1. Deep enrichment of secondary phases within the La Thuile soils

The Li isotope distribution in the soil profiles of the present-day La Thuile catchment highlights the influence of the formation of fine, clay-
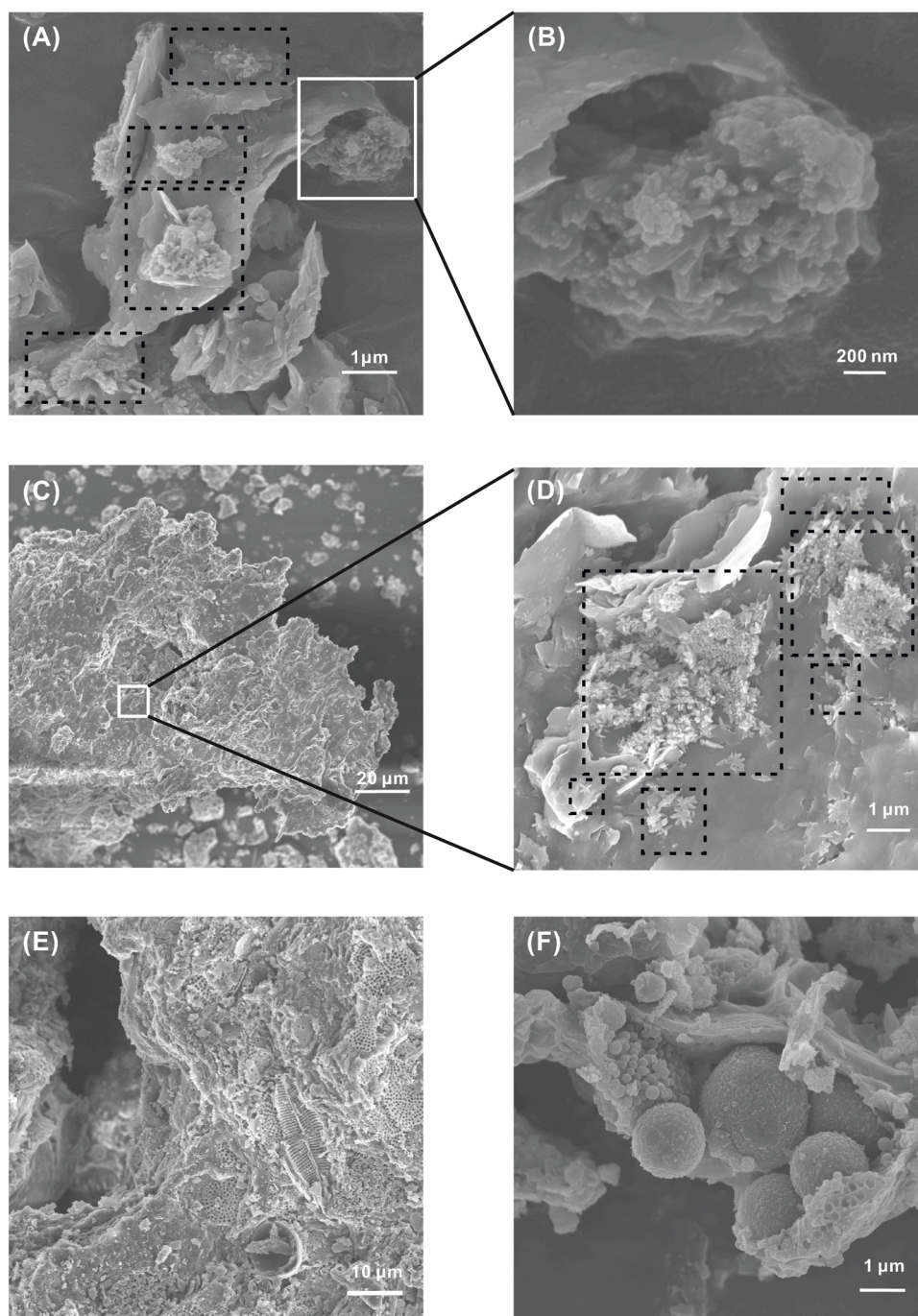
Fig 4. SEM images of (A) Soil sample THU02–3, 15–30 cm depth; (B) Magnified secondary mineral phases observed in (A); (C) Soil sample THU02–4, 30–80 cm depth; (D) Magnified secondary minerals attached to surface of large grain from (C); (E) Holocene lake sediment (THU10–02C1a-79–80) with grain surfaces dominated by bio-skeletons; and (F) Example of bio-skeleton. The white boxes denote the regions magnified. The black dashed boxes highlight the regions with the presence of fine-sized secondary phases.

rich particles during pedogenesis, implying their potential role in shaping the lake sediment composition over time. In these soil profiles, δ^7Li decreases with increasing depth and reaches values well below that of rock at the base of the soil profile. During chemical weathering, secondary minerals such as clays preferentially incorporate ^{6}Li (Hindshaw et al., 2019; Vigier et al., 2008). Consequently, δ^7Li in the soil solids or river sediments serves as a proxy for the extent of secondary mineral precipitation, with secondary minerals having lower δ^7Li compared to their source bedrock (Dellinger et al., 2014, 2017). Therefore, the low δ^7Li values at the base of the La Thuile soil profiles suggest that these profiles are enriched in secondary minerals at depth relative to topsoil horizons.

This enrichment of clay-rich particles in the present-day La Thuile deep soil horizons can be further investigated using the mass transfer coefficient value (τ), defined as:

$$\tau_{i,j} = \left(C_{j,w} \times C_{i,p}\right)/\left(C_{j,p} \times C_{i,w}\right) - 1 \qquad (2)$$

where i and j represent immobile and mobile elements, respectively, and w and p denote the element concentrations in the sample of interest and in the parent material (Brimhall and Dietrich, 1987; Nesbitt, 1979). Negative τ values indicate a loss of the mobile element, and positive values suggest a gain. In this study, Ti was selected as the immobile reference element, as it is one of the most immobile elements during weathering processes (Nesbitt, 1979). The downward increase in $\tau_{Ti,Al}$ values suggests a depletion of Al-rich phases at the soil surface and a likely enrichment of Al-rich phases in the deeper horizons of La Thuile soils (Fig. 2). In particularly, profile THU02 exhibits positive $\tau_{Ti,Al}$ values in the deepest soil horizons, which could suggest a net gain of Al in depth. Considering both δ^7Li and $\tau_{Ti,Al}$ (Fig. 2), it can be inferred that clay minerals are transported from shallower horizons and accumulated in deeper layers of La Thuile soils. In addition to the geochemical proxies, the presence of the clusters of fine particles is visually confirmed through imaging analysis of THU02 soil profile (Fig. 4). Scrutiny under SEM revealed only few secondary particles observed in the shallow soils. Nevertheless, in deeper horizons, fine secondary phases were identified based on mineral morphology and EDX analysis (Fig. 4A-4D). These sub-micron particles (Fig. 4B and 4D) are enriched in Al and Fe (Fig. S4). Notably, these secondary particles (<1 μm) appear to be coated/attached to larger-sized grains (>200 μm, Fig. 4C) rather than being present as individual grains. The fact that in the La Thuile soils these secondary phases are present as a "coating" on larger soil particles is further supported by leaching experiments (see leaching experiment section in supplementary material, Fig. S5). Such coatings were also observed in other studies (e.g. Kim et al., 2018). This aggregation is possibly caused by the fact that mineral surfaces control the growth/crystallization of new phases (King et al., 2010; Ruiz-Agudo et al., 2016). The downward movement of fine particles revealed by the geochemical and imaging results is not reflected in the grain size data (Fig. S2). This apparent discrepancy can first be explained by the challenges associated with the isolation of fine particles due to the coating effect. Second, while fine clay fractions can represent a significant fraction of a soil sample, direct quantification by laser diffraction method is difficult (Dur et al., 2004; Taubner et al., 2009).

This observed discrepancy between grain-size results and geochemical data highlights the importance of differentiating between clay-sized particles and clay minerals. Clay-sized particles are often isolated from soil and sediment samples to study weathering through sieving, settling, and/or chemical treatment. However, our findings suggest that such a procedure could introduce artefacts if larger grains, which may carry a significant portion of weathering products, are discarded, or if chemical treatments, such as using HCl to remove carbonate minerals (e.g., Yang et al., 2021), are applied, which can also effectively dissolve a fraction of the poorly crystallized neoformed secondary phases (see leaching experiment section in supplementary material, Figure S5 and S7). Therefore, we recommend that researchers cautiously consider the interchangeable use of clay-sized particles and clay minerals and carefully test sieving/leaching methods to achieve a more comprehensive understanding of soil and sediment particles.

Variations in Li geochemistry in La Thuile soils could be attributed to the vertical transfer of clay minerals as a chemical (dissolution-reprecipitation of clay minerals) and/or physical process (downward mobilization of clay particles). The dissolution-reprecipitation of clay minerals as suggested in the soils from the Strengbach Critical Zone Observatory (France; Lemarchand et al., 2010) could be a valid contender to explain the Li isotope and clay mineral mobilization in La Thuile. This mechanism entails clay minerals dissolution in the surficial horizons and reprecipitation at depth following downward percolation of solute-rich soil solutions. Such reprecipitation could lead to an accumulation of fine particles in deeper horizons (Brantley and White, 2009). Clay dissolution at the surface would release low δ^7Li signatures in the solution (Lemarchand et al., 2010; Zhang et al., 2021), resulting in the remaining solids having δ^7Li values close to that of bedrock. Conversely, the reprecipitation of secondary minerals from Al-rich and ^{6}Li-rich soil solutions would produce a low δ^7Li signal and high Al content at the bottom of the soil profile - both features being observed in the sample soils from La Thuile.

To examine further the roles of chemical and physical mobilization of Li within the La Thuile soils, we use a combination of different mass transfer coefficients. In CZ waters, nominally dissolved elements can be transported as ions ("truly dissolved") or carried by fine particles such as colloids or nanoparticles ("apparently dissolved"). Previous studies (Hasenmueller et al., 2017; Steinhoefel et al., 2021; Sullivan et al., 2016) have suggested that $\tau_{Ti,Li}$ could indicate the total Li mass transfer in both forms of Al-rich fine particles and solutes (both truly and apparently dissolved fractions), whereas $\tau_{Al,Li}$ strictly traces the loss of Li through solute export (truly dissolved only). Consequently, the difference between these two coefficients ($\tau_{Ti,Li}$- $\tau_{Al,Li}$) should reflect the Li loss by the export of particles (Steinhoefel et al., 2021). However, we note that a small fraction of Al may dissolve if clay dissolution is effective (Zhang et al., 2021), in which case the $\tau_{Al,Li}$ value provides a minimum estimate for the fraction of Li lost through chemical transfer in the dissolved phase. In the La Thuile soil profiles, Li is depleted in the soils, as most samples have negative $\tau_{Ti,Li}$ values (Fig. 2). Negative $\tau_{Ti,Li}$- $\tau_{Al,Li}$ values in the soil profiles, particularly in the upper horizons, imply that this export is occurring in the form of fine particles. At depth, the $\tau_{Ti,Li}$- $\tau_{Al,Li}$ values increase to values close to 0, indicating no loss and even an accumulation of fine particles there. Similar geochemical features are observed for other elements (Na, K, Mg, and Fe) in these two soil profiles (Fig. S8). Notably, the mass transfer coefficient proxy matches the microscope imaging results (Fig. 4). For samples with the calculated $\tau_{Ti,Li}$- $\tau_{Al,Li}$ significantly below 0, few secondary particles are observed, whereas when $\tau_{Ti,Li}$- $\tau_{Al,Li}$ is close to or greater than 0, secondary fine particles are clearly visible at the microscopic level.

The imaging results obtained from profile THU02 reveal that the presence of fine particles is limited to deep soil layers, and they exhibit better crystallization in the deepest horizon (Fig. 4D and S5B) compared to those found at shallower depths (Fig. 4B). Fine particles observed in deeper horizons have better defined morphology and are typically present as longer rods than in upper horizons. Here, we propose a scenario coupling the two mechanisms discussed above (dissolution-reprecipitation of clays and lessivage) to explain the La Thuile system (Fig. S9). At the soil surface dilute meteoric water dissolves minerals from marine sedimentary rocks, leading to the enrichment of dissolved clay-making solute such as Al in the fluid. As this solution percolates downward, permeability decreases, pH increases (Bajard et al., 2017a), and the formation of secondary phases is favoured, most likely first as amorphous material. Further downward fluid percolation results in the transport of these poorly-crystallized secondary phases. With later growth of these particles along the flow path (e.g., Caraballo et al., 2019; Gebauer et al., 2018), the accumulation of this secondary material might occur in lower-porosity, deep horizons. In this scenario, both chemical

transformation and physical transport of fine, secondary material contribute to the formation of a pool of fine particles that are readily mobilizable *via* water percolation, and which accumulate in deep soil horizon, leading to the observed δ^7Li decreases with depth.

To summarize, the present-day soil data in La Thuile show that soil Li concentrations and isotope profiles are not exclusively controlled by the formation of secondary minerals from parent materials in the topsoil, as in "classical" soil profiles (Golla et al., 2021; Rothacker et al., 2018). Instead, the Li profiles are better explained by the translocation of clay-rich fine particles from topsoils to deeper horizons (Figs. 4 and S9). Therefore, the Li isotope signature of topsoils is influenced not only by the extent of modern clay formation but also by the particle movement within the soil. Although illuviation is a well-known process in soil science (*e.g.*, Egli et al., 2006), the associated metal stable isotope effects are poorly understood. Addressing this knowledge gap can enhance our understanding of soil evolution in a wider variety of CZ environments. In the next section, we explore the potential impact of these soil processes on the interpretation of the geochemical signals from lake sediments.

5.2. The relative role of fine particle transport in determining the lake sediment composition

Variations in lake sediment δ^7Li have been previously attributed to the change in catchment soil processes, with the newly formed clay minerals carrying low δ^7Li signatures enriched within topsoils (Rothacker et al., 2018). However, it has also been recognized that the δ^7Li signature in lake sediments can be influenced by grain size (Weynell et al., 2017). The novel soil δ^7Li data presented in this study suggest that the formation of easily mobilizable, clay-rich, fine particles may impact the interpretation of the paleo-environmental signal preserved in the sediments. Consequently, a re-evaluation of the message conveyed by lake sediments becomes necessary.

When comparing La Thuile sediments and soils, it is noteworthy that the youngest sediment exhibits higher Al/Ti ratio and lower δ^7Li value than present-day surface soils (Table 1). This geochemical offset between deposited lake sediments and modern catchment soils may reflect (1) poor representation of the lake source materials in the studied soil profiles; (2) influence of lacustrine diagenetic processes on the sediment after deposition; (3) hydrological sorting of particles within the lake *i.e.,* preferential removal of small particles through the lake outflux; or (4) selective export of soil particles with distinct geochemical compositions (relative to bulk soil) to the lake.

A sediment source different from the studied soil profiles could result in the observed geochemical offset but is unlikely. First, the soil sample sites sit on steeper slopes and have greater erosion potentials than other parts of the catchment, making them likely major sources of sediment to the lake (Fig. 1). Second, dust inputs into Lake La Thuile are negligible (Giguet-Covex et al., 2019). Accordingly, similarities between lake sediments and soils in their ratios of immobile elements (REEs/Ti), which are not fractionated by weathering and sorting processes (Goldstein and Jacobsen, 1988; Nesbitt, 1979), suggest a common rock source (Fig. S3).

Diagenetic processes could modify the sedimentary geochemical signals including δ^7Li deposited in deltaic environments (Zhang et al., 2022). However, these processes typically occur in marine environments with Li-(and other cations)-rich saline water. Lake La Thuile is a proglacial lake whose aqueous chemistry and short water residence time are unlikely to experience such processes. As shown by Bajard et al. (2016), La Thuile sediments contain some proportions of authigenic components and organic matter, essentially carbonates and biogenic silica (diatoms). As these phases likely carry very low Li concentrations (Chan et al., 2006; Dellinger et al., 2018), their influence on Li isotopes can be neglected. However, we note that diagenetic processes do affect lake sediment grain size at La Thuile. Lake sediments from the mid-Holocene with clay-like geochemical signals have relatively large grain sizes (Bajard et al., 2016), which is opposite to previous observations in river

sediments (Dellinger et al., 2014). SEM examination of these lake sediments reveal that they are characterized by abundant biological materials, possibly cemented with authigenic carbonate (Fig. S6). This observation suggests in-lake interactions between biological and detrital materials decouples sediment geochemical signatures and grain size. Moreover, this observation implies that the "bulk" sedimentation rates from this period (Holocene climatic optimum) could lead to an overestimation of the erosion rates (Francke et al., 2022, 2020).

In-lake hydrodynamic sorting may affect lake sediment geochemistry as finer particles have greater potential to be transported by the lake outflux than coarser particles. At La Thuile, the ephemeral outflux may transport some sediments when the epilimnion flow is rapid/turbid, likely associated with episodes of high sedimentation rates during which hydrodynamic sorting is weakened. During low sedimentation periods, fine particles are likely to be retained by settlings and/or interaction with the lake biomass (Jones et al., 2014), which is abundant in La Thuile during such periods (Fig. 4E and 4F). Finally, the preferential removal of fine particles through the lake outflow would result in remaining sediments deposited at the lake bottom having elevated δ^7Li and reduced Al/Ti values compared to soils, which contrasts with our observations.

Therefore, we can eliminate causes (1), (2), and (3) cited above and infer that the differences between modern soils and recent lake sediments in the La Thuile catchment are likely due to the selective export of particles from soils, together with the possible selective transport thereof to the site of deposition.

Direct examination of selective sediment transport is difficult (Bern and Yesavage, 2018; Kim et al., 2018; Walling et al., 2002), and fluvial transport of fine particles is a complex process (Dietze et al., 2014; Juergen et al., 2007). Nonetheless, the export of clay-rich fine particles by subsurface flow has been demonstrated to be a significant process at the Shale Hills Critical Zone Observatory, a catchment underlain by shale rock (*e.g.,* Jin et al., 2010). Sedimentary column taken from deposits along the stream within the catchment have revealed an accumulation of fine particles resulting from catchment erosion (Ma et al., 2015). The selective transport of fine particles has also been observed during surface erosion driven by rainwater (Shi et al., 2012). During soil erosion and sorting in streams, this preferential transport effect could lead to an export of sediment dominated by fine particles rich in secondary phases and thus enriched in ^{6}Li (Steinhoefel et al., 2021; Weynell et al., 2017). In the following section, we discuss the variations in the geochemical record from the La Thuile sediment sequence in light of the possibility for selective export of fine particles as a significant soil and catchment process.

5.3. Refining the interpretation of the Lake La Thuile paleo-record using lithium isotopes

The importance of soil formation and selective transport of fine particles in the La Thuile catchment highlights the need to consider these processes when interpreting the sediment sequence in terms of local soil evolution and the corresponding weathering history (Fig. 3). As discussed above, Li isotope geochemistry in the La Thuile catchment is most likely associated with both secondary mineral formation during pedogenesis and selective transport of fine particles from soils. It is worth noting that these two processes are likely closely coupled, as both are sensitive to local modification in CZ functioning.

Broadly speaking, the relationships between δ^7Li, Al/Ti, and $\tau_{Ti,Li}$-$\tau_{Al,Li}$ (Fig. 5A and 5B) encompassing modern soils and lake sediments from different epochs (Late Glacial Period, Holocene-Middle Age, post-Middle Age) allow us to draw the main features of the past CZ evolution at La Thuile. The most notable observation is that the sediments with the lowest δ^7Li values (<-5‰), highest Al/Ti ratio, and highest $\tau_{Ti,Li}$-$\tau_{Al,Li}$ values are exclusively associated with low sedimentation rates (~ 0.1 mm/yr; Fig. S10). Such low sedimentation rates at La Thuile have been interpreted by previous studies as reflecting low catchment erosion
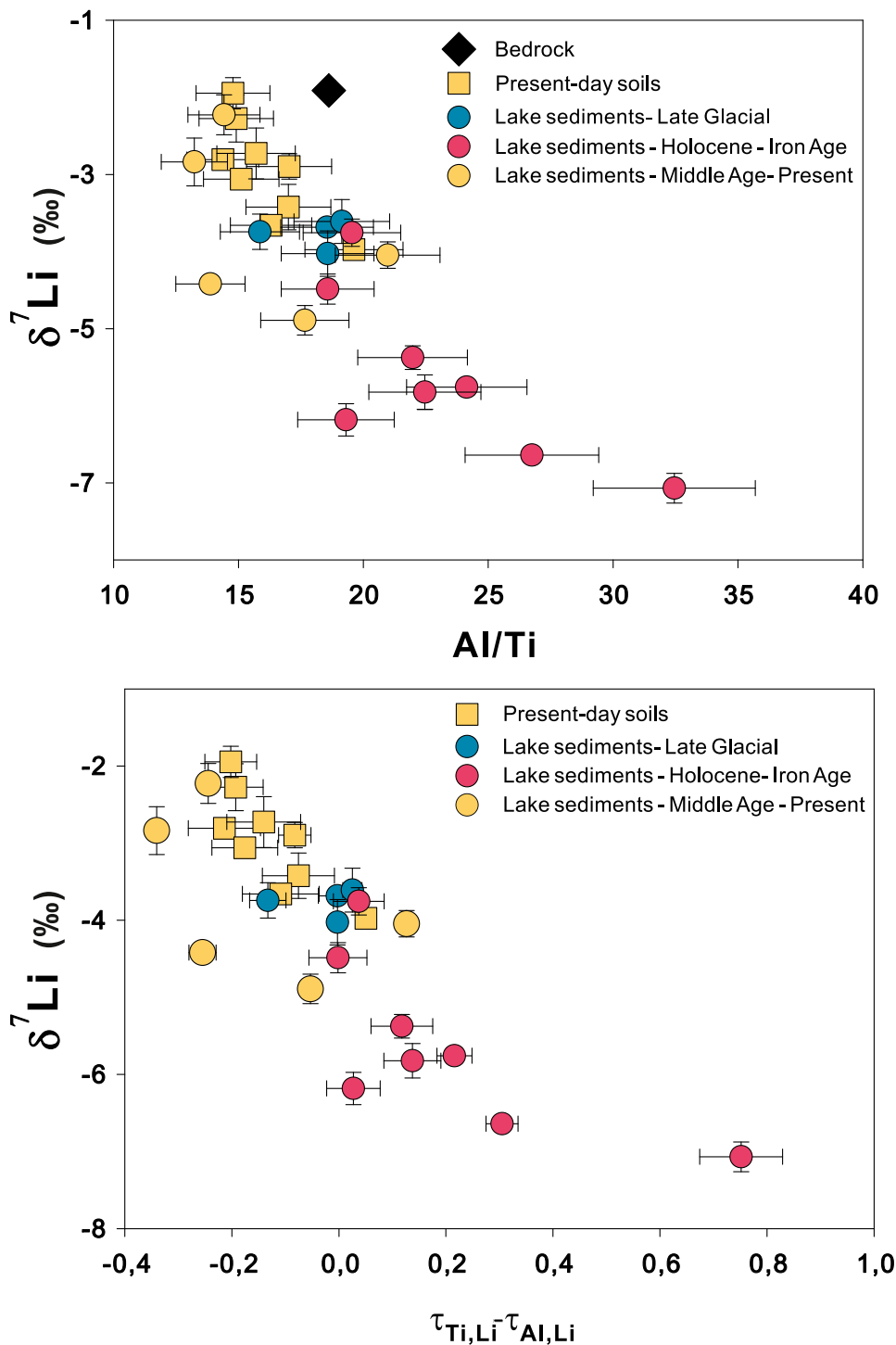
Fig 5. La Thuile soil and sediment Li isotope composition as a function of (A) Al/Ti and (B) $\tau_{Ti,Li}$- $\tau_{Al,Li}$.

rates concomitant with dense forest cover (Bajard et al., 2017a, 2016).

We can construct a historical scenario for Lake La Thuile using the δ^7Li record as a proxy of secondary minerals, and by examining the possible effects of selective transport with the $\tau_{Ti,Li}$-$\tau_{Al,Li}$ record. From the late Last Glacial Period to the onset of the Holocene (phase 1 in Fig. 3), the δ^7Li record is relatively constant and slightly enriched in ^{6}Li compared to the bedrock. This suggests the presence of pre-Holocene soils in the catchment, associated with moderate sedimentation rates and bedrock-like Al/Ti signatures. The $\tau_{Ti,Li}$-$\tau_{Al,Li}$ values of these sediments are close to 0, indicating no enrichment of fine particles. In essence, during this period unsorted soil surface material was

transported to the lake. These data suggest a scenario of limited soil development and sustained erosion, resulting in lake sediments having geochemical characteristics close to that of the bedrock.

Lake La Thuile sediments deposited between approximately 8000 and 3000 yr cal BP have lower δ^7Li values, down to ∼ −7.1 ‰, Al/Ti ratios higher than that of bedrock, and positive $\tau_{Ti,Li}$-$\tau_{Al,Li}$ values, up to 0.75. SEM analysis revealed the influence of lake aquatic biological activity during this period, as indicated by the presence of abundant bio-skeleton such as diatoms (Fig. 4E, 4F, and S6). However, there is no evidence suggesting that biological activity affected the Li-Al-Ti geochemistry as these elements are not nutrients. Therefore, we

propose that abiotic processes, such as clay formation and transport, were the primary drivers of the lake sediment signatures. The geochemical data indicate secondary formation (low δ^7Li values) and suggest the role of selective transport of fine particles (positive $\tau_{Ti,Li}$-$\tau_{Al,Li}$ values). The decrease in δ^7Li values (phase 2 in Fig. 3) is consistent with the stabilization of slopes and soil development across the catchment. This was likely due to a climate transition from the Late Glacial to the Holocene climatic optimum and drastic vegetation changes (Bajard et al., 2017a, 2016; Giguet-Covex et al., 2019). Pollen records (Bajard et al., 2016) illustrate denser vegetation in the catchment (Fig. 3E). Both warm climate and forest densification may have driven the observed reduced sedimentation rates at La Thuile, a feature also observed regionally in the Alps (Arnaud et al., 2012). This epoch marked a period of active soil horizon formation with diminished erosion rates (Fig. 3E). We note that these already-low erosion rates represent an upper-bound estimate due to the presence of authigenic (biological and carbonate) materials (Fig. S7), implying little detrital material was actually exported from the catchment. These conditions favoured both soil development - hence secondary mineral formation - and selective export of fine particles from soils, as witnessed by the sediment geochemical signatures. Essentially, the erosion flux associated with subsurface hydrological paths (spring, seeps, return flow, groundwater, etc.), where fine particles are preferentially transported (Morgan, 2009), played a more important role in the total erosion flux to the lake when surface soil erosion was restrained.

From 3000 to ~1600 yr cal BP (phase 3 in Fig. 3), we observe rising δ^7Li values and sedimentation rates and concomitant decreases in Al/Ti and $\tau_{Ti,Li}$-$\tau_{Al,Li}$ values. A previous investigation (Bajard et al., 2016) revealed the early human occupation of the watershed during this period, as shown by the increase in herbaceous pollen and the first appearance of *Cerealia* pollens. Our new dataset is consistent with the interpretation of increased erosion rates induced by human activities such as deforestation and agricultural practices at this time (Bajard et al., 2017a, 2016), suggesting early human activities modulated soil erosion mechanisms, including the role of selective export from soils and the transport of fine particles.

From 1600 yr cal BP to the beginning of the Medieval Warm Period (phase 4 in Fig. 3), a notable rise in sedimentation rate coincides with a sharp increase in δ^7Li values and reduced Al/Ti ratios. Negative $\tau_{Ti,Li}$-$\tau_{Al,Li}$ values suggest that selective transport of fine particles was not in operation at this time. Lake sediment geochemical signatures imply that material transported to the lake during this period closely resembled present-day topsoils. This observation can be explained by an increase in erosion rates with more pronounced human-induced agricultural activities. Therefore, the Li data from phase 4 imply that physical erosion was the major process shaping soil evolution in the catchment, supporting previous inferences (Bajard et al., 2017b). Little weathering signal can be observed from these sediments (*i.e.,* δ^7Li values from this period are close to bedrock), offering a milestone marking that humans have become the dominant control on CZ trajectories in the La Thuile catchment. During this period, lake sediments deposited can be regarded as a direct record for surface materials in the catchment area, encompassing both soils and exposed bedrock.

In the last millennium (phase 5), physical erosion rates first reached unprecedented values, signifying a paroxysmal period of soil destruction by human activities (Bajard et al., 2017a). Lake sediments from this period essentially represent unsorted eroded soils and rocks. The slight increase in $\tau_{Ti,Li}$-$\tau_{Al,Li}$ values (although still negative) and decrease in δ^7Li values observed in the lake sediments suggest an increasing contribution from relatively deep soil layers, likely associated with soil thinning due to enhanced agricultural activities. In other words, lower soil horizons formed during the Holocene pedologic optimum became exposed and were subject to erosion. Finally, after the erosion maximum of the Middle Ages, erosion rates decreased and agricultural activities reduced, allowing for soil redevelopment in the catchment (Bajard et al., 2017a, 2016). We can neglect the potential impact of industrial

fertilizers on the recent δ^7Li record, as fertilizers are typically highly soluble and exhibit heavy δ^7Li values (Négrel et al., 2010). As discussed earlier, the most recent lake sediments have a positive $\tau_{Ti,Li}$-$\tau_{Al,Li}$ value and a δ^7Li signature lower than that of present-day soils, suggesting that weathering and selective transport become active again in the catchment.

6. Conclusion and perspectives

In this article, we present soil and lake sediment Li isotopes from a pre-Alpine catchment underlain by calcareous rocks associated with shales. Our primary findings are that lake detrital sediment Li isotopes record distinct variations throughout the Late Glacial/Holocene periods and that humans have significantly altered the function of La Thuile CZ over the Holocene especially during the Middle Ages. We attributed these variations to changes in soil dynamics, erosion, and selective transport of fine particles across the catchment. Lake sediments have the potential to record the history of soil formation, but we show that these records are also dependent on several soil and catchment processes that might complicate their interpretation. In particular, the geochemical signature of weathering (characterized by low δ^7Li and high Al/Ti in sediments) is modulated in lake sediments as a result of both soil development and selective transport of fine particles.

This study illustrates the complex interplay of lithology, ecosystem development, climate, and human activities in shaping the CZ trajectory over time. In the La Thuile catchment underlain by sedimentary rocks, Li isotopes capture the multi-millennial formation of soils by chemical weathering and the importance of two contrasting physical processes: selective particle transport under low erosion rates and unsorted soil erosion under enhanced erosion periods, both intimately linked to landscape modifications driven by climate and human forcings. Together with previous studies on the fine particle flux transported by waters (Jin et al., 2010; Kim et al., 2018), our results of soil and sediment samples highlight the importance of differentiating between conflated terms such as "mobility" *vs.* "solubility" and "clay-sized particles" *vs.* "clay minerals (or more precisely, secondary phases, as amorphous materials do not qualify as clays)". These distinctions are critical for accurately recording and interpreting geochemical signatures.

To go beyond the horizon of our current understanding of CZ systems, particularly regarding the selective transport of fine particles, future studies are needed to focus on (1) better constraining sediment budgets; (2) gauging sediment fluxes associated with subsurface waters and outflows; (3) characterizing the geochemistry of detrital sediments as a function of grain size; (4) investigating the circumstances permitting for selective sediment transport in different geomorphic environments; and (5) characterizing the contribution of fine particles to the total detrital flux. It is undoubtedly challenging to separate fine particles from parent materials and to collect enough material for analysis. However, these challenges also present a valuable opportunity to investigate the properties and behaviours of these particles in nature, ultimately advancing our understanding of CZ processes.

CRediT authorship contribution statement

Xu (Yvon) Zhang: Methodology, Validation, Resources, Data curation, Investigation, Writing – original draft, Visualization. **Manon Bajard:** Methodology, Validation, Resources, Data curation, Investigation, Visualization, Writing – review & editing. **Julien Bouchez:** Validation, Supervision, Writing – review & editing, Funding acquisition. **Pierre Sabatier:** Conceptualization, Resources, Methodology, Data curation, Validation, Supervision, Writing – review & editing, Funding acquisition. **Jérôme Poulenard:** Resources, Methodology, Validation. **Fabien Arnaud:** Conceptualization, Resources, Data curation, Validation, Supervision, Writing – review & editing. **Christian Crouzet:** Data curation, Validation. **Marie Kuessner:** Data curation. **Mathieu**

Dellinger: Writing – review & editing. **Jérôme Gaillardet:** Conceptualization, Methodology, Validation, Supervision, Writing – review & editing, Visualization, Funding acquisition.

Declaration of Competing Interest

The authors declare that they have no known competing financial interests or personal relationships that could have appeared to influence the work reported in this paper.

Data availability

Data will be made available on request.

Acknowledgements

Supplementary materials

Supplementary material associated with this article can be found, in the online version, at doi:10.1016/j.epsl.2023.118463.

References

Arnaud, F., Révillon, S., Debret, M., Revel, M., Chapron, E., Jacob, J., Giguet-Covex, C., Poulenard, J., Magny, M., 2012. Lake Bourget regional erosion patterns reconstruction reveals Holocene NW European Alps soil evolution and paleohydrology. Quat. Sci. Rev. 51, 81–92. https://doi.org/10.1016/j.quascirev.2012.07.025.

Arnaud, F., Sabatier, P., 2022. Lakes As Recorders of Earth Surface Dynamics From Yearly to Plurimillennial Time-Scales, in: Mehner, T., Tockner, K.B.T.-E. of I.W. (Second E. (Eds.), Elsevier, Oxford, pp. 439–452. https://doi.org/10.1016/B978-0-12-819166-8.00125-0.

Bajard, M., Poulenard, J., Sabatier, P., Develle, A.-L., Giguet-Covex, C., Jacob, J., Crouzet, C., David, F., Pignol, C., Arnaud, F., 2017a. Progressive and regressive soil evolution phases in the Anthropocene. Catena (Amst.) 150, 39–52. https://doi.org/10.1016/j.catena.2016.11.001.

Bajard, M., Poulenard, J., Sabatier, P., Etienne, D., Ficetola, F., Chen, W., Gielly, L., Taberlet, P., Develle, A.-L., Rey, P.-J., Moulin, B., de Beaulieu, J.-L., Arnaud, F., 2017b. Long-term changes in alpine pedogenetic processes: effect of millennial agro-pastoralism activities (French-Italian Alps). Geoderma 306, 217–236. https://doi.org/10.1016/j.geoderma.2017.07.005.

Bajard, M., Sabatier, P., David, F., Develle, A.-L., Reyss, J.-L., Fanget, B., Malet, E., Arnaud, D., Augustin, L., Crouzet, C., Poulenard, J., Arnaud, F., 2016. Erosion record in Lake La Thuile sediments (Prealps, France): evidence of montane landscape dynamics throughout the Holocene. Holocene 26, 350–364. https://doi.org/10.1177/0959683615609750.

Banjan, M., Crouzet, C., Sabatier, P., Jomard, H., Bajard, M., Demory, F., Develle, A.-L., Jenny, J.-P., Fanget, B., Malet, E., Findling, N., Alain, P., Didier, J., Bichet, V., Clapot, S., Messager, E., 2023. Did the younger dryas to holocene climate transition favour high seismicity rates in the north-western Alps? Sedimentology 70, 538–568. https://doi.org/10.1111/sed.13050.

Bern, C.R., Chadwick, O.A., Hartshorn, A.S., Khomo, L.M., Chorover, J., 2011. A mass-balance model to separate and quantify colloidal and solute redistributions in soil. Chem. Geol. 282, 113–119. https://doi.org/10.1016/j.chemgeo.2011.01.014.

Bern, C.R., Yesavage, T., 2018. Dual-phase mass balance modeling of small mineral particle losses from sedimentary rock-derived soils. Chem. Geol. 476, 441–455. https://doi.org/10.1016/j.chemgeo.2017.11.040.

Brantley, S.L., White, A.F., 2009. Approaches to modeling weathered regolith. Rev. Mineral. Geochem. 70, 435–484. https://doi.org/10.2138/rmg.2009.70.10.

Brimhall, G.H., Dietrich, W.E., 1987. Constitutive mass balance relations between chemical composition, volume, density, porosity, and strain in metasomatic hydrochemical systems: results on weathering and pedogenesis. Geochim. Cosmochim. Acta 51, 567–587. https://doi.org/10.1016/0016-7037(87)90070-6.

Buol, S.W., Southard, R.J., Graham, R.C., McDaniel, P.A., 2011. Soil-Forming Processes. Soil Genesis and Classification. Wiley Online Books. https://doi.org/10.1002/9780470960622.ch5.

Caraballo, M.A., Wanty, R.B., Verplanck, P.L., Navarro-Valdivia, L., Ayora, C., Hochella, M.F., 2019. Aluminum mobility in mildly acidic mine drainage: interactions between hydrobasaluminite, silica and trace metals from the nano to the meso-scale. Chem. Geol. 519, 1–10. https://doi.org/10.1016/j.chemgeo.2019.04.013.

Chan, L., Leeman, W.P., Plank, T., 2006. Lithium isotopic composition of marine sediments. Geochem., Geophys., Geosyst. 7, Q06005. https://doi.org/10.1029/2005GC001202.

Dellinger, M., Bouchez, J., Gaillardet, J., Faure, L., Moreau, J., 2017. Tracing weathering regimes using the lithium isotope composition of detrital sediments. Geology 45, 411–414. https://doi.org/10.1130/G38671.1.

Dellinger, M., Gaillardet, J., Bouchez, J., Calmels, D., Galy, V., Hilton, R.G., Louvat, P., France-Lanord, C., 2014. Lithium isotopes in large rivers reveal the cannibalistic nature of modern continental weathering and erosion. Earth Planet. Sci. Lett. 401, 359–372. https://doi.org/10.1016/j.epsl.2014.05.061.

Dellinger, M., West, A.J., Paris, G., Adkins, J.F., Pogge von Strandmann, P.A.E., Ullmann, C.V., Eagle, R.A., Freitas, P., Bagard, M.-L., Ries, J.B., 2018. The Li isotope composition of marine biogenic carbonates: patterns and Mechanisms. Geochim. Cosmochim. Acta 236, 315–335. https://doi.org/10.1016/j.gca.2018.03.014.

Dietze, E., Maussion, F., Ahlborn, M., Diekmann, B., Hartmann, K., Henkel, K., Kasper, T., Lockot, G., Opitz, S., Haberzettl, T., 2014. Sediment transport processes across the Tibetan Plateau inferred from robust grain-size end members in lake sediments. Clim. Past 10, 91–106. https://doi.org/10.5194/cp-10-91-2014.

Dosseto, A., Vigier, N., Joannes-Boyau, R.C., Moffat, I., Singh, T., Srivastava, P., 2015. Rapid response of silicate weathering rates to climate change in the Himalaya. Geochem. Perspect. Lett. 1, 10–19. https://doi.org/10.7185/geochemlet.1502.

Dur, J.C., Elsass, F., Chaplain, V., Tessier, D., 2004. The relationship between particle-size distribution by laser granulometry and image analysis by transmission electron microscopy in a soil clay fraction. Eur. J. Soil Sci. 55, 265–270. https://doi.org/10.1111/j.1365-2389.2004.00597.x.

Egli, M., Mirabella, A., Sartori, G., Zanelli, R., Bischof, S., 2006. Effect of north and south exposure on weathering rates and clay mineral formation in Alpine soils. Catena (Amst.) 67, 155–174. https://doi.org/10.1016/j.catena.2006.02.010.

Francke, A., Dosseto, A., Forbes, M., Cadd, H., Short, J., Sherborne-Higgins, B., Constantine, M., Tyler, J., Tibby, J., Marx, S.K., Dodson, J., Mooney, S., Cohen, T.J., 2022. Catchment vegetation and erosion controlled soil carbon cycling in south-eastern Australia during the last two glacial-interglacial cycles. Glob. Planet Change 217, 103922. https://doi.org/10.1016/j.gloplacha.2022.103922.

Francke, A., Holtvoeth, J., Codilean, A.T., Lacey, J.H., Bayon, G., Dosseto, A., 2020. Geochemical methods to infer landscape response to Quaternary climate change and land use in depositional archives: a review. Earth Sci. Rev. 207, 103218 https://doi.org/10.1016/j.earscirev.2020.103218.

Gaillardet, J., Braud, I., Hankard, F., Anquetin, S., Bour, O., Dorfliger, N., de Dreuzy, J.R., Galle, S., Galy, C., Gogo, S., Gourcy, L., Habets, F., Laggoun, F., Longuevergne, L., Le Borgne, T., Naaim-Bouvet, F., Nord, G., Simonneaux, V., Six, D., Tallec, T., Valentin, C., Abril, G., Allemand, P., Arènes, A., Arfib, B., Arnaud, L., Arnaud, N., Arnaud, P., Audry, S., Comte, V.B., Batiot, C., Battais, A., Bellot, H., Bernard, E., Bertrand, C., Bessière, H., Binet, S., Bodin, J., Bodin, X., Boithias, L., Bouchez, J., Boudevillain, B., Moussa, I.B., Branger, F., Braun, J.J., Brunet, P., Caceres, B., Calmels, D., Cappelaere, B., Celle-Jeanton, H., Chabaux, F., Chalikakis, K., Champollion, C., Copard, Y., Cotel, C., Davy, P., Deline, P., Delrieu, G., Demarty, J., Dessert, C., Dumont, M., Emblanch, C., Ezzahar, J., Estèves, M., Favier, V., Faucheux, M., Filizola, N., Flammarion, P., Floury, P., Fovet, O., Fournier, M., Francez, A.J., Gandois, L., Gascuel, C., Gayer, E., Genthon, C., Gérard, M.F., Gilbert, D., Gouttevin, I., Grippa, M., Gruau, G., Jardani, A., Jeanneau, L., Join, J.L., Jourde, H., Karbou, F., Labat, D., Lagadeuc, Y., Lajeunesse, E., Lastennet, R., Lavado, W., Lawin, E., Lebel, T., Le Bouteiller, C., Legout, C., Lejeune, Y., Le Meur, E., Le Moigne, N., Lions, J., Lucas, A., Malet, J.P., Marais-Sicre, C., Maréchal, J.C., Marlin, C., Martin, P., Martins, J., Martinez, J.M., Massei, N., Mauclerc, A., Mazzilli, N., Molénat, J., Moreira-Turcq, P., Mougin, E., Morin, S., Ngoupayou, J.N., Panthou, G., Peugeot, C., Picard, G., Pierret, M.C., Porel, G., Probst, A., Probst, J.L., Rabatel, A., Raclot, D., Ravanel, L., Rejiba, F., René, P., Ribolzi, O., Riotte, J., Rivière, A., Robain, H., Ruiz, L., Sanchez-Perez, J.M., Santini, W., Sauvage, S., Schoeneich, P., Seidel, J.L., Sekhar, M., Sengtaheuanghoung, O., Silvera, N., Steinmann, M., Soruco, A., Tallec, G., Thibert, E., Lao, D.V., Vincent, C., Viville, D., Wagnon, P., Zitouna, R., 2018. OZCAR: the French network of critical zone observatories. Vadose Zone J. 17, 180067 https://doi.org/10.2136/vzj2018.04.0067.

Gebauer, D., Raiteri, P., Gale, J.D., Cölfen, H., 2018. On classical and non-classical views on nucleation. Am. J. Sci. 318, 969. https://doi.org/10.2475/09.2018.05.

Georg, R.B., Reynolds, B.C., Frank, M., Halliday, A.N., 2006. New sample preparation techniques for the determination of Si isotopic compositions using MC-ICPMS. Chem. Geol. 235, 95–104. https://doi.org/10.1016/j.epsl.2006.07.006.

Gibbard, P., Walker, M., Bauer, A., Edgeworth, M., Edwards, L., Ellis, E., Finney, S., Gill, J.L., Maslin, M., Merritts, D., Ruddiman, W., 2022. The anthropocene as an event, not an epoch. J. Quat. Sci. 37, 395–399. https://doi.org/10.1002/jqs.3416.

Giguet-Covex, C., Ficetola, G.F., Walsh, K., Poulenard, J., Bajard, M., Fouinat, L., Sabatier, P., Gielly, L., Messager, E., Develle, A.L., David, F., Taberlet, P., Brisset, E., Guiter, F., Sinet, R., Arnaud, F., 2019. New insights on lake sediment DNA from the catchment: importance of taphonomic and analytical issues on the record quality. Sci. Rep. 9, 14676. https://doi.org/10.1038/s41598-019-50339-1.

Goldstein, S.J., Jacobsen, S.B., 1988. Rare earth elements in river waters. Earth Planet. Sci. Lett. 89, 35–47. https://doi.org/10.1016/0012-821X(88)90031-3.

Golla, J.K., Kuessner, M.L., Henehan, M.J., Bouchez, J., Rempe, D.M., Druhan, J.L., 2021. The evolution of lithium isotope signatures in fluids draining actively weathering hillslopes. Earth Planet. Sci. Lett. 567, 116988 https://doi.org/10.1016/j.epsl.2021.116988.

Hasenmueller, E.A., Gu, X., Weitzman, J.N., Adams, T.S., Stinchcomb, G.E., Eissenstat, D. M., Drohan, P.J., Brantley, S.L., Kaye, J.P., 2017. Weathering of rock to regolith: the activity of deep roots in bedrock fractures. Geoderma 300, 11–31. https://doi.org/10.1016/j.geoderma.2017.03.020.

Hindshaw, R.S., Tosca, R., Goût, T.L., Farnan, I., Tosca, N.J., Tipper, E.T., 2019. Experimental constraints on Li isotope fractionation during clay formation. Geochim. Cosmochim. Acta 250, 219–237. https://doi.org/10.1016/j.gca.2019.02.015.

Huh, Y., Chan, L.-H., Zhang, L., Edmond, J.M., 1998. Lithium and its isotopes in major world rivers: implications for weathering and the oceanic budget. Geochim. Cosmochim. Acta 62, 2039–2051. https://doi.org/10.1016/S0016-7037(98)00126-4.

Jenny, J.-P., Koirala, S., Gregory-Eaves, I., Francus, P., Niemann, C., Ahrens, B., Brovkin, V., Baud, A., Ojala, A.E.K., Normandeau, A., Zolitschka, B., Carvalhais, N., 2019. Human and climate global-scale imprint on sediment transfer during the Holocene. Proc. Natl. Acad. Sci. 116, 22972. https://doi.org/10.1073/pnas.1908179116. LP –22976.

Jin, L., Ravella, R., Ketchum, B., Bierman, P.R., Heaney, P., White, T., Brantley, S.L., 2010. Mineral weathering and elemental transport during hillslope evolution at the Susquehanna/Shale Hills Critical Zone Observatory. Geochim. Cosmochim. Acta 74, 3669–3691. https://doi.org/10.1016/j.gca.2010.03.036.

Jones, J.I., Duerdoth, C.P., Collins, A.L., Naden, P.S., Sear, D.A., 2014. Interactions between diatoms and fine sediment. Hydrol. Process 28, 1226–1237. https://doi.org/10.1002/hyp.9671.

Juergens, S., John, S., Kevin, T., 2007. Accretion of mudstone beds from migrating floccule ripples. Science 318 (1979), 1760–1763. https://doi.org/10.1126/science.1147001.

Kim, H., Gu, X., Brantley, S.L., 2018. Particle fluxes in groundwater change subsurface shale rock chemistry over geologic time. Earth Planet. Sci. Lett. 500, 180–191. https://doi.org/10.1016/j.epsl.2018.07.031.

King, H.E., Plümper, O., Putnis, A., 2010. Effect of secondary phase formation on the carbonation of olivine. Environ. Sci. Technol. 44, 6503–6509. https://doi.org/10.1021/es9038193.

Kuessner, M.L., Gourgiotis, A., Manhès, G., Bouchez, J., Zhang, X., Gaillardet, J., 2020. Automated analyte separation by ion chromatography using a Cobot applied to geological reference materials for Li isotope composition. Geostand. Geoanal. Res. https://doi.org/10.1111/ggr.12295.

Lemarchand, E., Chabaux, F., Vigier, N., Millot, R., Pierret, M.-C., 2010. Lithium isotope systematics in a forested granitic catchment (Strengbach, Vosges Mountains, France). Geochim. Cosmochim. Acta. https://doi.org/10.1016/j.gca.2010.04.057.

Ma, L., Teng, F.-Z., Jin, L., Ke, S., Yang, W., Gu, H.-O., Brantley, S.L., 2015. Magnesium isotope fractionation during shale weathering in the Shale Hills Critical Zone Observatory: accumulation of light Mg isotopes in soils by clay mineral transformation. Chem. Geol. 397, 37–50. https://doi.org/10.1016/j.chemgeo.2015.01.010.

McLaren, P., Bowles, D., 1985. The effects of sediment transport on grain-size distributions. Journal of Sedimentary Research 55, 457–470. https://doi.org/10.1306/212F86FC-2B24-11D7-8648000102C1865D.

Montgomery, D.R., 2007. Dirt: The Erosion of Civilizations. University of California Press, 1st ed.

Morgan, R.P.C., 2009. Soil Erosion and Conservation. John Wiley & Sons, 3rd Editio. ed.

Nantke, C.K.M., Brauer, A., Frings, P.J., Czymzik, M., Hübener, T., Stadmark, J., Dellwig, O., Roeser, P., Conley, D.J., 2021. Human influence on the continental Si budget during the last 4300 years: δ30Sidiatom in varved lake sediments (Tiefer See, NE Germany). Quat. Sci. Rev. 258, 106869 https://doi.org/10.1016/j.quascirev.2021.106869.

Négrel, P., Millot, R., Brenot, A., Bertin, C., 2010. Lithium isotopes as tracers of groundwater circulation in a peat land. Chem. Geol. 276, 119–127. https://doi.org/10.1016/j.chemgeo.2010.06.008.

Nesbitt, H.W., 1979. Mobility and fractionation of rare earth elements during weathering of a granodiorite. Nature 279, 206–210. https://doi.org/10.1038/279206a0.

Noireaux, J., Sullivan, P.L., Gaillardet, J., Louvat, P., Steinhoefel, G., Brantley, S.L., 2021. Developing boron isotopes to elucidate shale weathering in the critical zone. Chem. Geol. 559, 119900 https://doi.org/10.1016/j.chemgeo.2020.119900.

Pogge von Strandmann, P.A.E., Kasemann, S.A., Wimpenny, J.B., 2020. Lithium and lithium isotopes in earth's surface cycles. Elements 16, 253–258. https://doi.org/10.2138/gselements.16.4.253.

Quénard, L., Samouëlian, A., Laroche, B., Cornu, S., 2011. Lessivage as a major process of soil formation : a revisitation of existing data. Geoderma 135–147. https://doi.org/10.1016/j.geoderma.2011.07.031, 167–168.

Rapuc, W., Arnaud, F., Sabatier, P., Anselmetti, F.S., Piccin, A., Peruzza, L., Bastien, A., Augustin, L., Régnier, E., Gaillardet, J., von Grafenstein, U., 2022. Instant sedimentation in a deep Alpine lake (Iseo, Italy) controlled by climate, human and geodynamic forcing. Sedimentology 69, 1816–1840. https://doi.org/10.1111/sed.12972.

Roattino, T., Crouzet, C., Vassallo, R., Buoncristiani, J.-F., Carcaillet, J., Gribenski, N., Valla, P.G., 2022. Paleogeographic reconstruction of the western French Alps foreland during the last glacial maximum using cosmogenic exposure dating. Quat. Res. 1–16. https://doi.org/10.1017/qua.2022.25.

Rothacker, L., Dosseto, A., Francke, A., Chivas, A.R., Vigier, N., Kotarba-Morley, A.M., Menozzi, D., 2018. Impact of climate change and human activity on soil landscapes

over the past 12,300 years. Sci. Rep. 8, 247. https://doi.org/10.1038/s41598-017-18603-4.

Ruddiman, W.F., 2013. The Anthropocene. Annu. Rev. Earth Planet. Sci. 41, 45–68. https://doi.org/10.1146/annurev-earth-050212-123944.

Rudnick, R.L., Tomascak, P.B., Njo, H.B., Gardner, L.R., 2004. Extreme lithium isotopic fractionation during continental weathering revealed in saprolites from South Carolina. Chem. Geol. 212, 45–57. https://doi.org/10.1016/j.chemgeo.2004.08.008.

Ruiz-Agudo, E., King, H.E., Patiño-López, L.D., Putnis, C.V., Geisler, T., Rodriguez-Navarro, C., Putnis, A., 2016. Control of silicate weathering by interface-coupled dissolution-precipitation processes at the mineral-solution interface. Geology 44, 567–570. https://doi.org/10.1130/G37856.1.

Shi, Z.H., Fang, N.F., Wu, F.Z., Wang, L., Yue, B.J., Wu, G.L., 2012. Soil erosion processes and sediment sorting associated with transport mechanisms on steep slopes. J. Hydrol. (Amst.) 454–455, 123–130. https://doi.org/10.1016/j.jhydrol.2012.06.004,

Song, Y., Zhang, X.Y., Bouchez, J., Chetelat, B., Gaillardet, J., Chen, J., Zhang, T., Cai, H., Yuan, W., Wang, Z., 2021. Deciphering the signatures of weathering and erosion processes and the effects of river management on Li isotopes in the subtropical Pearl River basin. Geochim. Cosmochim. Acta 313, 340–358. https://doi.org/10.1016/j.gca.2021.08.015.

Steffen, W., Rockström, J., Richardson, K., Lenton, T.M., Folke, C., Liverman, D., Summerhayes, C.P., Barnosky, A.D., Cornell, S.E., Crucifix, M., Donges, J.F., Fetzer, I., Lade, S.J., Scheffer, M., Winkelmann, R., Schellnhuber, H.J., 2018. Trajectories of the earth system in the anthropocene. Proc. Natl. Acad. Sci. 115, 8252. https://doi.org/10.1073/pnas.1810141115. LP –8259.

Steinhoefel, G., Brantley, S.L., Fantle, M.S., 2021. Lithium isotopic fractionation during weathering and erosion of shale. Geochim. Cosmochim. Acta 295, 155–177. https://doi.org/10.1016/j.gca.2020.12.006.

Stephens, L., Fuller, D., Boivin, N., Rick, T., Gauthier, N., Kay, A., Marwick, B., Armstrong, C.G., Barton, C.M., Denham, T., Douglass, K., Driver, J., Janz, L., Roberts, P., Rogers, J.D., Thakar, H., Altaweel, M., Johnson, A.L., Sampietro Vattuone, M.M., Aldenderfer, M., Archila, S., Artioli, G., Bale, M.T., Beach, T., Borrell, F., Braje, T., Buckland, P.I., Jiménez Cano, N.G., Capriles, J.M., Diez Castillo, A., Çilingiroğlu, Ç., Negus Cleary, M., Conolly, J., Coutros, P.R., Covey, R. A., Cremaschi, M., Crowther, A., Der, L., di Lernia, S., Doershuk, J.F., Doolittle, W.E., Edwards, K.J., Erlandson, J.M., Evans, D., Fairbairn, A., Faulkner, P., Feinman, G., Fernandes, R., Fitzpatrick, S.M., Fyfe, R., Garcea, E., Goldstein, S., Goodman, R.C., Dalpoim Guedes, J., Herrmann, J., Hiscock, P., Hommel, P., Horsburgh, K.A., Hritz, C., Ives, J.W., Junno, A., Kahn, J.G., Kaufman, D., Kearns, C., Kidder, T.R., Lanoë, F., Lawrence, D., Lee, G.-A., Levin, M.J., Lindskoug, H.B., López-Sáez, J.A., Macrae, S., Marchant, R., Marston, J.M., McClure, S., McCoy, M.D., Miller, A.V., Morrison, M., Motuzaite Matuzeviciute, G., Müller, J., Nayak, A., Noerwidi, S., Peres, T.M., Peterson, C.E., Proctor, L., Randall, A.R., Renette, S., Robbins Schug, G., Ryzewski, K., Saini, S., Scheinsohn, V., Schmidt, P., Sebillaud, P., Seitsonen, O., Simpson, I.A., Sołtysiak, A., Speakman, R.J., Spengler, R.N., Steffen, M.L., Storozum, M.J., Strickland, K.M., Thompson, J., Thurston, T.L., Ulm, S., Ustunkaya, M.C., Welker, M.H., West, C., Williams, P.R., Wright, D.K., Wright, N., Zahir, M., Zerboni, A., Beaudoin, E., Munevar Garcia, S., Powell, J., Thornton, A., Kaplan, J.O., Gaillard, M.-J., Klein Goldewijk, K., Ellis, E., 2019. Archaeological assessment reveals Earth's early transformation through land use. Science 365 (1979), 897. https://doi.org/10.1126/science.aax1192. LP –902.

Sullivan, P.L., Hynek, S.A., Gu, X., Singha, K., White, T., West, N., Kim, H., Clarke, B., Kirby, E., Duffy, C., Brantley, S.L., 2016. Oxidative dissolution under the channel leads geomorphological evolution at the Shale Hills catchment. Am. J. Sci. 316, 981. https://doi.org/10.2475/10.2016.02. LP –1026.

Taubner, H., Roth, B., Tippkötter, R., 2009. Determination of soil texture: comparison of the sedimentation method and the laser-diffraction analysis. J. Plant Nutr. Soil Sci. 172, 161–171. https://doi.org/10.1002/jpln.200800085.

Vigier, N., Decarreau, A., Millot, R., Carignan, J., Petit, S., France-Lanord, C., 2008. Quantifying Li isotope fractionation during smectite formation and implications for the Li cycle. Geochim. Cosmochim. Acta 72, 780–792. https://doi.org/10.1016/j.gca.2007.11.011.

Walling, D.E., Russell, M.A., Hodgkinson, R.A., Zhang, Y., 2002. Establishing sediment budgets for two small lowland agricultural catchments in the UK. Catena (Amst.) 47, 323–353. https://doi.org/10.1016/S0341-8162(01)00187-4.

Weynell, M., Wiechert, U., Schuessler, J.A., 2017. Lithium isotopes and implications on chemical weathering in the catchment of Lake Donggi Cona, northeastern Tibetan Plateau. Geochim. Cosmochim. Acta. https://doi.org/10.1016/j.gca.2017.06.026.

Wirsig, C., Zasadni, J., Christl, M., Akçar, N., Ivy-Ochs, S., 2016. Dating the onset of LGM ice surface lowering in the High Alps. Quat. Sci. Rev. 143, 37–50. https://doi.org/10.1016/j.quascirev.2016.05.001.

Yang, C., Vigier, N., Yang, S., Revel, M., Bi, L., 2021. Clay Li and Nd isotopes response to hydroclimate changes in the Changjiang (Yangtze) basin over the past 14,000 years. Earth Planet. Sci. Lett. 561, 116793 https://doi.org/10.1016/j.epsl.2021.116793.

Zhang, X.Y., Gaillardet, J., Barrier, L., Bouchez, J., 2022. Li and Si isotopes reveal authigenic clay formation in a palaeo-delta. Earth Planet. Sci. Lett. 578, 117339 https://doi.org/10.1016/j.epsl.2021.117339.

Zhang, X.Y., Saldi, G.D., Schott, J., Bouchez, J., Kuessner, M., Montouillout, V., Henehan, M., Gaillardet, J., (Yvon) Zhang, X., Saldi, G.D., Schott, J., Bouchez, J., Kuessner, M., Montouillout, V., Henehan, M., Gaillardet, J., 2021. Experimental constraints on Li isotope fractionation during the interaction between kaolinite and seawater. Geochim. Cosmochim. Acta 292, 333–347. https://doi.org/10.1016/j.gca.2020.09.029.